

Synthesis and Characterization of ZP-4 (KZnPO₄·0.8H₂O), a New Zincophosphate Microporous Material: Structure Solution from a 2.5 × 2.5 × 8 μm Single Crystal Using a Third Generation Synchrotron X-ray Source

R. W. Broach,* R. L. Bedard, and S. G. Song

UOP LLC, 50 East Algonquin Road, Des Plaines, Illinois 60017

J. J. Pluth

Department of Geophysical Sciences, Center for Advanced Radiation Sources, Geological/Soil/Environmental, and Materials Research Science and Engineering Center, 5734 South Ellis Avenue, University of Chicago, Chicago, Illinois 60637

A. Bram, C. Riekel, and H.-P. Weber

European Synchrotron Radiation Facility, BP 220, 38043, Grenoble, France

Received December 28, 1998. Revised Manuscript Received April 29, 1999

New techniques for handling crystals and collecting data allow structure solution from micrometer-sized crystals. Our experience using these techniques for determining the crystal structure of ZP-4 (KZnPO₄·0.8H₂O), a new potassium zincophosphate microporous material, is described. Crystals were mounted using a micromanipulator attached to a Nikon optical microscope. Data on a 2.5 × 2.5 × 8 μm single crystal were collected at Beamline Insertion Device 13 at the European Synchrotron Radiation Facility (ESRF). Lattice constants of the orthorhombic cell in space group *Ccc2* are $a = 13.812(3)$, $b = 13.836(3)$, and $c = 13.134(3)$ Å. The structure refined to a final $R1 = 0.0680$ using all 1876 reflections. The structure of ZP-4 is similar to the naturally occurring zeolite edingtonite (structure type EDI). It consists of a four-connected three-dimensional framework of alternating Zn and P tetrahedra producing a three-dimensional eight-ring channel system. The channels are nearly circular along the *a*- and *b*-axis directions, but are elliptical along *c*. The structure is disordered and was modeled by adding a second component to the single-crystal refinement. Electron diffraction spots reveal streaking along the [100] direction and weak systematic absence violations consistent with a disordered model involving EDI/THO intergrowths.

Introduction

Structure determination from powder samples was revolutionized by the availability of second-generation synchrotron sources. These sources, such as the National Synchrotron Light Source (NSLS) at Brookhaven National Laboratory in New York, facilitated collection of high-resolution powder diffraction data, allowing successful intensity extraction, ab initio structure solution, and subsequent Rietveld refinement. A new generation of dedicated synchrotron sources, such as the European Synchrotron Radiation Facility (ESRF) in Grenoble, France, the Advanced Photon Source (APS) in Argonne, IL, and the Super Photon Ring-8 in Harima Science Garden City, Japan, provide intensities and beam qualities that permit various types of microanalysis, including crystal structure determinations from micrometer-sized crystals. It is now possible to select single crystals from powder samples (even impure samples) for data collection and structure solution.¹

Our attempts at structure solution of a new zincophosphate molecular sieve from high-resolution powder data were unsuccessful because of ambiguity in the symmetry and because of severe overlap of reflections due to the similarity of the three orthorhombic lattice parameters. For that reason single-crystal data on a tiny crystal were collected at the ESRF. The synthesis, characterization, and structure solution are reported here.

A large number of aluminophosphate-based molecular sieves have been synthesized and reported.^{2–7} Many of these molecular sieves have frameworks without zeolite analogues. More recently, other-metal phosphate-based

(1) Harding, M. M. *J. Synchrotron Rad.* **1996**, *3*, 250.

(2) Wilson, S. T.; Lok, B. M.; Messina, C. A.; Cannon, T. R.; Flanigen, E. M. *ACS Symp. Ser.* **1983**, *218*, 79.

(3) Flanigen, E. M.; Patton, R. L.; Wilson, S. T. *Stud. Surf. Sci. Catal.* **1988**, *37*, 13.

(4) Wilson, S. T.; Lok, B. M.; Messina, C. A.; Cannon, T. R.; Flanigen, E. M. *J. Am. Chem. Soc.* **1982**, *104*, 1146.

(5) Flanigen, E. M.; Lok, B. M.; Patton, R. L.; Wilson, S. T. *Pure Appl. Chem.* **1986**, *10*, 1351.

(6) Wilson, S. T. *Stud. Surf. Sci. Catal.* **1991**, *58*, 137.

(7) Bennett, J. M.; Dytrych, W. J.; Pluth, J. J.; Richardson, J. W., Jr.; Smith, J. V. *Zeolites* **1986**, *6*, 349.

molecular sieves have been reported.^{8–15} Zincophosphate materials synthesized in our labs have been designated ZP-*n*. For example, we have synthesized ZP-1, which has the same topology^{8,14} as the zeolite sodalite, and ZP-2, which has the same topology^{8,10,13} as the zeolite Li-A(BW). ZP-3 does not have a zeolite analogue^{8,15} and is related to the pharmacosiderite family of octahedral/tetrahedral networks. ZP-5 is an open-framework zincophosphate with a new chiral tetrahedral framework topology.^{8,9} Reported here are the synthesis and characterization of ZP-4, whose topology remained unknown until we were able to collect synchrotron single-crystal data of sufficiently high quality to permit structure solution using a very small crystal.

Experimental Section

Synthesis and Initial Characterization. A reaction mixture was prepared by combining 40 g of $K_2HPO_4 \cdot xH_2O$, 20 g of $ZnCl_2$, 20 g of KCl, and 2 L of H_2O . A few drops of 85% H_3PO_4 were added to clarify the solution, followed by rapid addition of 200 mL of 0.1 M KOH. The pH was further adjusted to a final value of 9.6 by the addition of 167.2 g of diethyl-ethanolamine. The reaction mixture was stirred for 18 h at room temperature (about 20 °C). The product was isolated by filtration, washed with distilled water, and dried in air at room temperature. X-ray powder diffraction indicated the product was pure and highly crystalline. The empirical formula, $KZnPO_4 \cdot 0.8H_2O$, was determined from elemental analysis by ICP (ZnO 38.60 wt %, P_2O_5 33.80 wt %, K_2O 22.80 wt %) and loss on ignition, LOI (6.90 wt %).

Adsorption studies with a McBain Bakr gravimetric apparatus indicated reversible adsorption of H_2O but no adsorption of larger molecules, suggesting a small six- to eight-ring pore-size material. The adsorption studies as well as thermogravimetric and DTA studies revealed the crystals collapse at approximately 330 °C. We did not investigate the effects of synthesis parameters on degree of intergrowth.

Single-Crystal Structure Solution and Refinement. For the X-ray diffraction studies, a single crystal with dimensions $2.5 \times 2.5 \times 8 \mu m$ was mounted on a glass capillary tapered to about $1 \mu m$. Crystal selection and mounting was facilitated by using a Nikon microscope equipped with a micromanipulator. Single-crystal data were collected on a κ -geometry diffractometer at the ESRF.¹⁶ An X-ray beam from an undulator was focused to $30 \mu m$ by an ellipsoidal mirror, and monochromatized to 0.6883 \AA (18 keV) by a channel-cut Si(111) crystal cooled by liquid nitrogen. Seventy-three frames were collected on a charge-coupled area detector (11-cm fluorescent screen with lens coupling) by rotating φ 10° in 20 s.

Reduction of the CCD single-crystal data was accomplished using the DENZO program.¹⁷ Intensities were extracted from the frames using a primitive cell which was later transformed to a C-centered orthorhombic unit cell with $a = 13.812(3) \text{ \AA}$, b

Table 1. Crystal Data and Structure Refinement for ZP-4

empirical formula	$KZnPO_4 \cdot 0.8H_2O$
formula weight	213.85 Daltons
temperature	295(2) K
wavelength	0.68830 \AA
crystal system	orthorhombic
space group	$Ccc2$; #37
unit cell dimensions	$a = 13.812(3) \text{ \AA}$, $\alpha = 90^\circ$; $b = 13.836(3) \text{ \AA}$, $\beta = 90^\circ$; $c = 13.134(3) \text{ \AA}$, $\gamma = 90^\circ$
volume, Z	$2509.9(9) \text{ \AA}^3$, 20
density (calculated)	2.830 g/cm^3
absorption coefficient	5.958 mm^{-1}
$F(000)$	2080
crystal size	$0.080 \times 0.025 \times 0.025 \text{ mm}$
θ range for data collection	$4.04\text{--}27.17^\circ$
limiting indices	$-16 \leq h \leq 16$, $-16 \leq k \leq 16$, $-11 \leq l \leq 11$
reflections collected	4133
independent reflections	1876 [$R(\text{int}) = 0.0697$]
refinement method	full-matrix least-squares on F^2
data/restraints/parameters	1834/1/199
goodness-of-fit on F^2	1.014
final R indices [$I > 2\sigma(I)$]	$R1 = 0.0581$, $wR2 = 0.1512$
R indices (all data)	$R1 = 0.0680$, $wR2 = 0.1706$
absolute structure parameter	0.44(4)
extinction coefficient	0.0009(4)
largest diff. peak and hole	1.636 and -0.830 e\AA^{-3}

$= 13.836(3) \text{ \AA}$, $c = 13.134(3) \text{ \AA}$, and $V = 2509.9(9) \text{ \AA}^3$ in space group $Ccc2$. SHELXTL¹⁸ yielded solution and refinement of the structure using 4133 reflections merged to 1876 unique reflections ($R_{\text{merge}} = 0.0697$). After all unique atoms were located in the unit cell, a difference Fourier map revealed large residual peaks at unreasonably close distances to other atoms. These peaks were related to other atoms by a mirror plane normal to the c axis and result from disorder (as described below). After an appropriate shift of the origin along the c axis to put the mirror at $z = 0$, the K, Zn, and P disordered atoms were added. For each K, Zn, or P atom with fractional coordinates x, y, z , a mirror related atom was added with fractional coordinates $x, y, -z$. In further refinements, the fractional coordinates for mirror related atoms were constrained to conform to the mirror. At this point, the refinement converged (R_1 all data = 0.0680). Overall occupancy factors for the original and mirror atoms (which were allowed to vary with the constraint that the sum be 1.0) refined to 0.835(6) and 0.165(6). Attempts to add the appropriate mirror-related O-atoms did not improve the refinement. No further large residual peaks were found in a final difference Fourier. Details of the structure refinement are given in Table 1.

TEM Studies. TEM samples of ZP-4 were prepared by dispersing crystal particles on a honeycomb carbon grid using ethanol. The JEOL 2000FX microscope was operated at 200 kV. Attempts to obtain a lattice image of the crystals were not successful because of the sensitivity of the sample to the convergent beam. The material is stable to investigation by on-zone selected area electron diffraction (SAD).

Results

Structure of ZP-4. Atomic coordinates, selected interatomic distances and angles, and anisotropic displacement parameters for the unique set of atoms are given in Tables 2–4. To a first approximation, ZP-4 has the topology of structure type EDI.¹⁹ Thus its framework structure is similar to the naturally occurring zeolite edingtonite^{20,21,22} and the synthetic zeolites K–F,^{23,24,25}

(8) Bedard, R. L. U.S. Patent 5302362, April 12, 1994. Bedard, R. L. U.S. Patent 5126120, June 30, 1992.

(9) Harrison, W. T. A.; Gier, T. E.; Stucky, G. D.; Broach, R. W.; Bedard, R. L. *Chem. Mater.* **1996**, *8*, 145.

(10) Gier, T. E.; Stucky, G. D. *Nature* **1991**, *349*, 508.

(11) Xu, R.; Chen, J.; Feng, C. *Stud. Sur. Sci. Catal.* **1991**, *60*, 63.

(12) Harrison, W. T. A.; Martin, T. E.; Gier, T. E.; Stucky, G. D. *J. Mater. Chem.* **1992**, *2*, 175.

(13) Harrison, W. T. A.; Gier, T. E.; Nicol, J. M.; Stucky, G. D. *J. Solid State Chem.* **1995**, *114*, 249.

(14) Nenoff, T. N.; Harrison, W. T. A.; Gier, T. E.; Stucky, G. D. *J. Am. Chem. Soc.* **1991**, *113*, 378.

(15) Harrison, W. T. A.; Broach, R. W.; Bedard, R. L.; Gier, T. E.; Bu, X.; Stucky, G. D. *Chem. Mater.* **1996**, *8*, 691.

(16) Neder, R. B.; Burghammer, M.; Grasl, T.; Schulz, H.; Bram, A.; Fiedler, S.; Riekel, C. *Z. Kristallogr.* **1996**, *211*, 763.

(17) Otwinowski, Z. in *Data Collection and Processing*; Sawyer, L., Isaacs, N., Bailey, S., Eds.; Daresbury Lab.: Warrington, U.K., 1993; pp 56–62.

(18) Sheldrick, G. M. *SHELXTL, Program for the Solution and Refinement of Crystal Structures*; Bruker AXS, Inc., Analytical X-ray Systems, Madison, WI, 1993.

(19) Meier, W. M.; Olson, D. H.; Baerlocher, Ch. *Atlas of Zeolite Structure Types. Zeolites* **1996**, *17*.

Table 2. Atomic Coordinates ($\text{\AA} \times 10^4$), Equivalent Isotropic Displacement Parameters ($\text{\AA}^2 \times 10^3$), and Site Occupancy Factors (sof) for ZP-4^a

atom	x	y	z	U(eq)	sof
Zn(1)	7673(1)	3733(1)	89(2)	27(1)	1.0
Zn(2)	8734(1)	7673(1)	1210(1)	21(1)	1.0
Zn(3)	7500	7500	8156(2)	23(1)	0.5
P(1)	7727(2)	6073(2)	-30(4)	23(1)	1.0
P(2)	8934(2)	7727(2)	6372(3)	16(1)	1.0
P(3)	7500	7500	3166(6)	22(1)	0.5
O(1)	8839(6)	7000(7)	5505(8)	35(3)	1.0
O(2)	8116(5)	4963(4)	5011(14)	44(3)	1.0
O(3)	6763(7)	6420(6)	6209(9)	37(2)	1.0
O(4)	7111(8)	6649(8)	3816(10)	49(3)	1.0
O(5)	7002(7)	6172(6)	805(10)	47(3)	1.0
O(6)	6414(5)	8254(5)	76(10)	30(2)	1.0
O(7)	6631(9)	7842(8)	2521(10)	45(3)	1.0
O(8)	9968(5)	8117(6)	6324(15)	50(4)	1.0
O(9)	7218(7)	6314(7)	8953(11)	45(4)	1.0
O(10)	8654(8)	7214(7)	7401(10)	40(3)	1.0
K(1)	7486(6)	61(4)	7506(7)	133(4)	1.0
K(2)	60(4)	7672(11)	8841(8)	177(7)	1.0
K(3)	5000	5000	1178(24)	118(11)	0.25(2)
K(4)	-79(39)	5116(39)	5059(26)	76(10)	0.28(1)
OW(1)	5241(19)	5030(27)	2385(45)	35(11)	0.25(2)
OW(2)	-70(40)	5251(35)	6491(52)	57(16)	0.22(1)

^a U(eq) is defined as one-third of the trace of the orthogonalized U_{ij} tensor. Positional parameters without an estimated standard deviation (number in parentheses) were not varied. Each atom has a corresponding disordered member (see text) with positional coordinates $x, y, -z$. The sof in the table have been normalized to 1.0 for the ordered component. The refined values for the sof of the ordered and disordered components were 0.835(6) and 0.165(6).

Table 3. Anisotropic Displacement Parameters ($\text{\AA}^2 \times 10^3$) for KZnPO_4 ^a

	U_{11}	U_{22}	U_{33}	U_{23}	U_{13}	U_{12}
Zn(1)	26(1)	16(1)	40(1)	1(1)	1(1)	1(1)
Zn(2)	11(1)	24(1)	27(1)	0(1)	-1(1)	0(1)
Zn(3)	22(1)	23(1)	25(2)	0	0	0(1)
P(1)	22(1)	12(1)	36(3)	3(2)	1(1)	0(1)
P(2)	5(1)	22(1)	20(3)	-3(1)	-4(1)	0(1)
P(3)	29(2)	25(2)	12(5)	0	0	1(2)
O(1)	32(5)	42(5)	31(9)	-11(4)	3(4)	3(4)
O(2)	25(4)	10(3)	96(10)	1(5)	9(6)	-3(3)
O(3)	41(5)	33(4)	35(8)	-2(5)	-1(5)	23(4)
O(4)	68(7)	44(5)	36(10)	0(5)	8(5)	4(5)
O(5)	38(5)	33(5)	69(11)	16(5)	21(5)	16(4)
O(6)	32(4)	22(4)	35(7)	4(4)	-12(4)	-11(3)
O(7)	60(7)	57(6)	19(10)	-2(5)	-3(6)	9(5)
O(8)	15(4)	20(5)	117(13)	-1(6)	-4(5)	-8(3)
O(9)	39(5)	36(5)	59(12)	-1(5)	-21(5)	-5(4)
O(10)	66(7)	42(5)	13(11)	1(4)	0(5)	13(5)
K(1)	330(13)	34(2)	34(6)	1(2)	12(7)	8(4)
K(2)	22(2)	464(23)	46(7)	34(9)	-9(2)	-34(5)
K(3)	140(17)	24(6)	189(27)	0	0	21(6)
K(4)	5(15)	55(25)	169(16)	-12(14)	-3(11)	14(11)

^a The anisotropic displacement factor exponent takes the form: $-2\pi^2 [h^2 a^{*2} U_{11} + \dots + 2hka^* b^* U_{12}]$.

Linde F,²⁶ and $\text{K}_2\text{Al}_2\text{Si}_3\text{O}_{10} \cdot \text{KCl}$.²⁷ The basic polyhedral building unit in ZP-4, containing six tetrahedral atoms, is the di-edge-stellated tetrahedron (des)²⁸ with the face

- (20) Mazzi, F.; Galli, E.; Gottardi, N. *N. Jb. Miner. Mh.* **1984**, 373.
 (21) Kvik, A.; Smith, J. V. *J. Chem. Phys.* **1983**, *79*, 2356.
 (22) Galli, E. *Acta Crystallogr.* **1976**, *B32*, 1623.
 (23) Barrer, R. M.; Baynham, J. W. *J. Chem. Soc.* **1956**, 2882.
 (24) Baerlocher, Ch.; Barrer, R. M. *Z. Kristallogr.* **1974**, *140*, 10.
 (25) Tambuyzer, E.; Bosmans, E. J. *Acta Crystallogr.* **1976**, *B32*, 1714.
 (26) Sherman, J. D. Proc. 4th IZC, Chicago. *ACS Symp. Ser.* **1977**, *40*, 30.
 (27) Ghose, S.; Hexiong, Y.; Weidner, J. R. *Am. Mineral.* **1990**, *75*, 947.
 (28) Smith, J. V. *Chem. Rev.* **1988**, *88*, 149–182.

Table 4. Selected Interatomic Distances (\AA) and Angles (deg) for ZP-4

Zn Tetrahedra		P Tetrahedra	
Zn(1)–O(1)	1.980(9)	P(1)–O(2)	1.532(7)
Zn(1)–O(2)	1.909(6)	P(1)–O(5)	1.491(11)
Zn(1)–O(3)	1.948(11)	P(1)–O(6)	1.515(7)
Zn(1)–O(4)	1.917(14)	P(1)–O(9)	1.545(13)
Zn(2)–O(5)	1.966(8)	P(2)–O(1)	1.525(10)
Zn(2)–O(6)	1.976(10)	P(2)–O(3)	1.538(8)
Zn(2)–O(7)	1.931(13)	P(2)–O(8)	1.528(8)
Zn(2)–O(8)	1.902(8)	P(2)–O(10)	1.574(12)
Zn(3)–O(9) $\times 2$	1.985(11)	P(3)–O(4) $\times 2$	1.551(13)
Zn(3)–O(10) $\times 2$	1.918(11)	P(3)–O(7) $\times 2$	1.544(13)
mean	1.944(32)	mean	1.536(21)
T–O–T Angles			
O(1)–Zn(1)–O(2)	103.8(4)	O(2)–P(1)–O(5)	107.2(7)
O(1)–Zn(1)–O(3)	105.1(4)	O(2)–P(1)–O(6)	107.3(4)
O(1)–Zn(1)–O(4)	115.4(5)	O(2)–P(1)–O(9)	113.1(8)
O(2)–Zn(1)–O(3)	110.5(5)	O(5)–P(1)–O(6)	113.7(7)
O(2)–Zn(1)–O(4)	110.1(6)	O(5)–P(1)–O(9)	108.1(7)
O(3)–Zn(1)–O(4)	111.5(5)	O(6)–P(1)–O(9)	107.6(6)
O(5)–Zn(2)–O(6)	105.7(4)	O(1)–P(2)–O(3)	110.4(6)
O(5)–Zn(2)–O(7)	114.0(5)	O(1)–P(2)–O(8)	106.4(7)
O(5)–Zn(2)–O(8)	104.3(4)	O(1)–P(2)–O(10)	108.9(6)
O(6)–Zn(2)–O(7)	113.9(5)	O(3)–P(2)–O(8)	107.9(5)
O(6)–Zn(2)–O(8)	111.5(5)	O(3)–P(2)–O(10)	108.2(6)
O(7)–Zn(2)–O(8)	107.1(7)	O(8)–P(2)–O(10)	115.1(8)
O(9)–Zn(3)–O(9)	116.3(7)	O(4)–P(3)–O(4)	113.2(11)
O(9)–Zn(3)–O(10) $\times 2$	105.4(5)	O(4)–P(3)–O(7) $\times 2$	105.4(7)
O(9)–Zn(3)–O(10) $\times 2$	106.3(5)	O(4)–P(3)–O(7) $\times 2$	109.8(7)
O(10)–Zn(3)–O(10)	117.8(8)	O(7)–P(3)–O(7)	113.4(11)
K–O Distances ($<3.4 \text{\AA}$)			
K(1)–O(9)	2.72(2)	K(3)–OW(1) $\times 2$	1.62(6)
K(1)–O(5)	2.803(14)	K(3)–O(8) $\times 2$	2.613(9)
K(1)–O(4)	2.846(14)	K(3)–O(3) $\times 2$	3.129(9)
K(1)–O(3)	2.859(12)	K(3)–O(5)	3.243(11)
K(1)–O(7)	3.132(14)	K(4)–OW(2)	1.89(7)
K(1)–OW(1)	3.14(3)	K(4)–OW(2)	1.96(7)
K(1)–O(2)	3.38(2)	K(4)–O(2)	2.50(6)
K(1)–O(2)	3.40(2)	K(4)–O(2)	2.71(5)
K(2)–O(10)	2.78(2)	K(4)–O(1)	3.06(4)
K(2)–O(1)	2.829(13)	K(4)–O(6)	3.06(7)
K(2)–O(7)	2.87(2)	K(4)–O(6)	3.17(7)
K(2)–O(6)	2.901(12)		
K(2)–O(4)	2.984(14)		
K(2)–O(8)	3.32(2)		
K(2)–O(8)	3.36(2)		

symbol, 4^4 . These des units link by sharing vertexes to form one-dimensional chains (designated **fib**²⁸) along the c axis with a repeat distance of about 6.6 \AA (Figure 1). Chains link parallel to the ab plane to form the three-dimensional EDI structure type. The distance from one chain to the next is about 6.9 \AA . In ZP-4, the a and b axes are double the chain distance, and the c -axis length is double the des repeat distance to accommodate the Zn and P ordering, rotation of the **fib** chains, and cation positioning.

The resulting four-connected three-dimensional framework of alternating Zn and P tetrahedra in ZP-4 produces a three-dimensional eight-ring channel system. The channels are nearly circular along the a - and b -axis directions, but are elliptical along c due to the rotation of the **fib** chains (Figures 2 and 3). The ellipticity along c is commonly, but not always, found in EDI-type zeolites. The angle of rotation of the **fib** chains, which is an index of the amount of distortion,

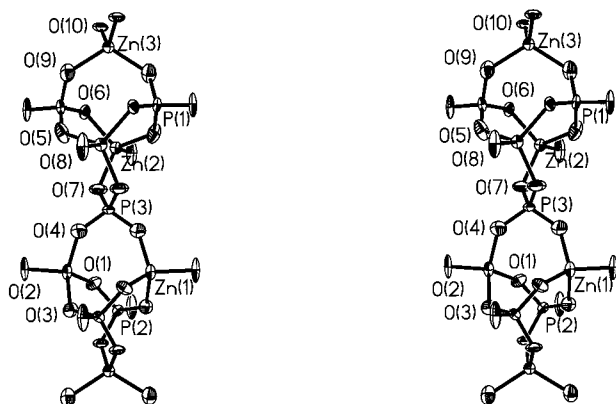


Figure 1. Stereoview of two linked di-edge-stellated tetrahedron (des) polyhedral building units in ZP-4. The des polyhedral building unit contains six tetrahedral atoms. The des units link by sharing vertexes to form one-dimensional chains (designated **fib**) along the *c* axis (vertical in the figure) with a repeat distance of about 6.6 Å.

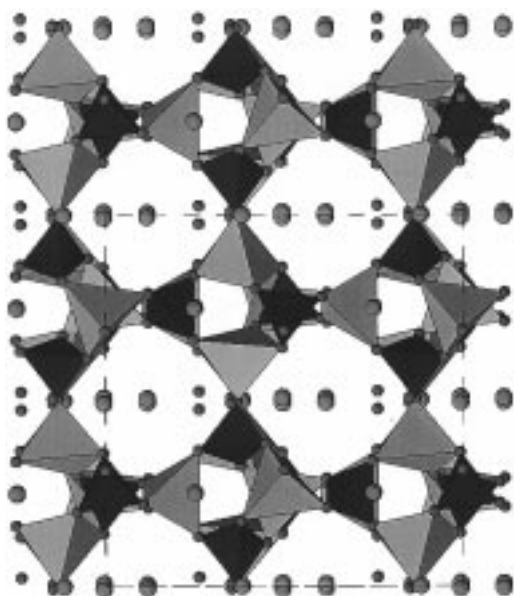


Figure 2. Projection of the ZP-4 structure showing the near circular eight-rings in the [010] direction and positions of the cations (larger circles) and water molecules (smaller circles). The unit cell is outlined and the *a* axis is vertical. ZnO_4 and PO_4 tetrahedra are shown as polyhedral units.

in two natural edingtonites is reported^{20,22} to be about 17°. The angle of rotation in ZP-4 (defined as $1/2$ the $\text{O}(2)\text{--O}(2)\text{--O}(2)$ or the $\text{O}(8)\text{--O}(8)\text{--O}(8)$ angle between chains) is about 14°.

Potassium atoms and water molecules occupy sites in the channels (Figure 2). K(1) and K(2) occupy sites near the centers of the eight-ring pores along the *a*- and *b*-axis channels and coordinate to oxygen atoms around the eight-ring pores. These sites are fully occupied. K(3) and K(4) are located in alternate channels along the *c* axis and also are sited near the centers of the eight-ring pores. These sites are only partially occupied (about one-half full), perhaps because oxygen atoms in the ellipsoidal rings are in less favorable positions for coordination. Out of the plane of the eight-rings, the potassium cations are presumably coordinated to water, not all of which was found in this study.

Defects that produce disorder in crystals of ZP-4 were suspected from the single-crystal studies and later

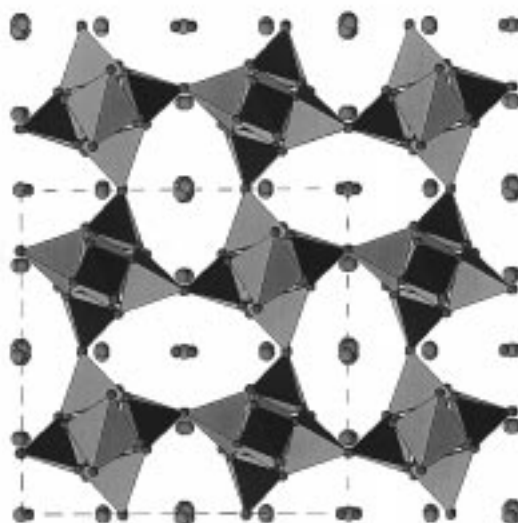


Figure 3. Projection of the ZP-4 structure showing the elliptical eight-rings in the [001] direction and positions of the cations (larger circles) and water molecules (smaller circles). The unit cell is outlined and the *b* axis is vertical. ZnO_4 and PO_4 tetrahedra are shown as polyhedral units.

confirmed by TEM analyses. The defects are related to the three alternative ways of linking **fib** chains parallel to the *ab* plane.²⁹ One way is to connect the chains such that neighboring des units have the same orientation along *c*; the four neighboring chains around a square face in a *c*-axis projection will all be oriented the same way (uuuu where u = up). The resulting three-dimensional topology is structure type EDI. If the chains are connected such that every other layer of chains in the *ab* plane is inverted (uudd in the square face where d = down), the resulting three-dimensional topology is structure type THO. Finally, if chain orientations are alternated (udud), the resulting topology is structure type NAT.

The model used in the single-crystal refinements is consistent with defects caused by inversion of some (about 16% based on the refinements) of the chains. It does not distinguish among the different ways the inverted chains could be arranged. There could be random inversions of single chains throughout the crystals (EDI/NAT faults), there could be random inversions across a plane (EDI/THO faults), or there could be regions in the crystals which have NAT or THO topologies (EDI/NAT or EDI/THO intergrowths).

TEM Analysis of Stacking Faults in ZP-4. TEM analysis was done in order to provide more insight into the type of defect in single crystals of ZP-4. Selected area electron diffraction (SAD) patterns from two different single crystals are shown in Figure 4. Two features are evident from the patterns; streaking along the [100] direction and weak violations of the systematic absences for C-centering.

The streaking provides information about the type of faulting in ZP-4. The zone axes of parts a and b of Figure 4 are [010] and $[0\bar{1}1]$, respectively. Both SADs exhibit streaking along [100] consistent with faulting on the

(29) Ross, M.; Flohr, M. J. K.; Ross, D. R. *Am. Mineral.* **1992**, *77*, 685.

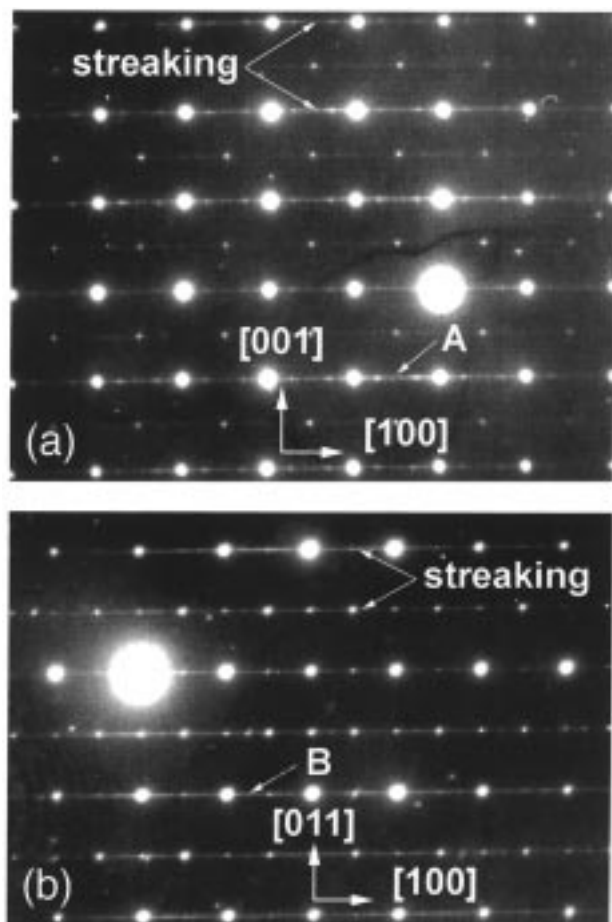


Figure 4. Selected area electron diffraction (SAD) patterns from two different single crystals with zone axes (a) [010] and (b) [011]. Two features are evident from the patterns; streaking along the [100] direction and weak violations of the systematic absences for C-centering.

(100) planes. The spots are not elongated vertically, indicating that faulting occurs only on the (100) planes, and not on the (010). This result suggests that faulting occurs on one of the two planes (100) and (010), and not simultaneously on both. Once a stacking fault is established on a particular plane of a crystal, it occurs repeatedly on the same set of planes resulting in a consistent faulting pattern throughout the crystal. This streaking pattern is consistent with faulting which occurs by inversion of planes of **fib** chains along the [100] direction (either EDI/THO faults or EDI/THO intergrowths).

The appearance of weak violations of the systematic absences for C-centering is most consistent with EDI/THO intergrowths, since it implies there are regions of the crystals which have a primitive unit cell (as does THO).

A close examination of Figure 4a shows that the streaking has certain fine structure, as indicated by "A" in the SAD pattern. The streaking is not continuous but rather discrete. The spacing of the fine spots can be related to the average thickness of the faulted plates, each being a perfect crystal of its own. Since the faulting occurs randomly, the plate thickness may change from one crystal to another, or even within a crystal. The spacing of the fine spots at "A" implies the plates in this crystal are on average ~ 60 Å thick. The streaking of

Figure 4b is more continuous than that in Figure 4a, suggesting a much smaller thickness of faulted plates in this crystal.

Bright field image of TEM did not reveal any stacking fault contrast. This may be explained by a low stacking fault energy. Since the displacement of atoms across the stacking faults occurs only at the second neighbor position, a low stacking fault energy is expected for the defect. This also explains the small stacking fault spacing implied by the continuous streaking of Figure 4b.

Discussion

The application of microcrystallography and complementary TEM studies successfully provided details of the structure of ZP-4 and the nature of the disorder. ZP-4 was shown to have the topology of structure type EDI¹⁹ to a first approximation. The structure contains a four-connected three-dimensional framework of alternating Zn and P tetrahedra. The framework defines a three-dimensional eight-ring channel system, occupied by potassium cations and water molecules. The channels are nearly circular along the *a*- and *b*-axis directions, but are elliptical along *c*.

The single-crystal X-ray refinements are consistent with a disordered structure in which regions of the crystal have **fib** chains inverted (faults or intergrowths). The selected area electron diffraction patterns suggest the disorder is best described as EDI/THO intergrowths.

This work demonstrates the power of new generation dedicated synchrotron sources for single-crystal data collection and analysis using very small crystals. High-quality data can be collected and structures solved from micrometer-sized and probably submicrometer-sized crystals. Neder et al. were able to collect single-crystal data and refine the structure from kaolinite crystals of 0.4 to $8 \mu\text{m}^3$ in size.¹⁶ The first example of a new mineral structure determination using synchrotron radiation was raite done at the ESRF using half of a needle $3 \times 3 \times 65 \mu\text{m}$ in size.³⁰ This capability allows more detailed structural information than can be obtained from Rietveld analysis for materials which are only available as micrometer-sized single crystals. Numerous applications are expected in the future, including structure solution of the numerous natural minerals only available in small crystals, structural details in materials where disorder and faulting precludes the growth of large crystals, and structure–performance relationships for industrially important catalysts and adsorbents where crystal size is often kept small to enhance diffusion.

Acknowledgment. We thank Professor Richard M. Kirchner of Manhattan College and Professor Joseph V. Smith of the University of Chicago for technical discussions of this work.

Supporting Information Available: Observed and calculated structure factors for ZP-4. This material is available free of charge via the Internet at <http://pubs.acs.org>.

CM9811444

(30) Pluth, J. J.; Smith, J. V.; Pushcharovsky, D. Y.; Semenov, E. I.; Bram, E. I.; Riekel, C.; Weber, H.-P.; Broach, R. W. *Proc. Natl. Acad. Sci.* **1998**, *94*, 12263.